Journal of Applied Polymer Science

Preparation and Properties of Modified Bismaleimide Resins Based on Phthalide-Containing Monomer

Xuhai Xiong,[1] Rong Ren,[1] Ping Chen,[1,2] Qi Yu,[1] Jing Wang,[1] Caixia Jia[1]

[1]Liaoning Key Laboratory of Advanced Polymer Matrix Composites Manufacturing Technology, College of Aerospace Engineering, Shenyang Aerospace University, Shenyang 110136, China

[2]State Key Laboratory of Fine Chemicals, School of Chemical Engineering, Dalian University of Technology, Dalian 116012, China

Correspondence to: P. Chen (E-mail: chenping_898@126.com).

ABSTRACT: A series of bismaleimide resins based on phthalide-containing monomer have been prepared by the copolymerization reaction of 3,3-bis[4-(4-maleimidophenoxy)phenyl] -phthalide (PPBMI), 4, 4'-dimaleimido diphenylmethane (MBMI) and 2, 2'-diallyl bisphenol A (DABPA) in different feed ratios. The curing behavior, thermal, mechanical and physical properties and compatibility of all resultant resins were carefully characterized using differential scanning calorimetry (DSC), thermogravimetric analysis (TGA), dynamic mechanical analysis (DMA), notched Izod impact test, water absorption test and scanning electron microscopy (SEM). DSC investigations showed that with an increase of the weight ratio of PPBMI, the dominating exothermic polymerization temperature (T_p) increased. The glass transitions were observed from DMA thermograms for the cured BMI resins in the temperature range from 277°C to 311°C and decreased with increasing PPBMI content. The TGA results indicated the thermal stability was improved as PPBMI content increased. The investigations of the mechanical properties showed a complicated trend with an increase in PPBMI content. In addition, the equilibrium water uptake of the modified resins was reduced as PPBMI content increased. © 2013 Wiley Periodicals, Inc. J. Appl. Polym. Sci. 130: 1084–1091, 2013

KEYWORDS: crosslinking; polyimides; kinetics

Received 3 December 2012; accepted 10 March 2013; Published online 17 April 2013
DOI: 10.1002/app.39269

INTRODUCTION

The development of high-performance polymer matrices has become the major driving force for the advanced lightweight composites. Bismaleimide (BMI) resins, a promising class of thermosetting polymers, attract considerable attention due to a combination of their exceptional processability prior to curing, low volumetric shrinkage on curing, and superior mechanical strength, excellent chemical and corrosion resistance, good dimensional stability, low moisture absorption and high service temperature after curing.[1,2] The above features make them widespread applications in aerospace industry and other high-tech fields.

However, the aromatic nature and the high crosslink density of the network result in an inherent brittleness of the cured virgin BMI resins. In the past three decades, the toughness improvement of BMI resins has been the focus of considerable interest and several approaches have been developed to overcome this drawback. Based on the difference of toughening mechanism, the modification methods are divided into three categories: (i) the incorporation of a second microphase of a dispersed elastomer, e.g.,[3,4] or a thermoplastic polymer, e.g.[5,6]; (ii) decreasing the crosslink density through Michael addition with active hydrogen atom-containing compounds, e.g., diamine,[7–9] dithiol,[10] aminobenzhydrazide,[2] copolymerization with allyl-terminated compound,[11–13] or design and synthesis of novel chain-extended BMI monomer[14–17]; (iii) cocuring with other thermosetting resins, e.g., epoxy,[18–20] cyanate ester,[21,22] benzoxazine.[23] Compared with other modifications, the copolymerization with allyl-substituted aromatic compounds may be the most preferred method for BMI modification. It not only could be able to enhance the toughness of BMIs but also endowed the modified resins with better process flexibility and lower cost. Based on 4,4'-bismaleimidodiphenyl methane (MBMI) and 2,2'-diallyl bisphenol A (DABPA), numerous high performance modified BMI resins were developed, such as QY8911-I, Matrimid 5292 and BASF 5260.[1,2,24] And the cure kinetics and mechanism of BMPM/DABPA systems were also investigated in detail using remote *in situ* real time fiber optic near-infrared spectroscopy, FTIR, fluorescence, UV-reflectance spectroscopy and other analytical techniques.[13,24–26] Despite the DABPA modified MBMI resins win great honors for their outstanding properties, the toughness of MBMI/DABPA is still not satisfactory for

© 2013 Wiley Periodicals, Inc.

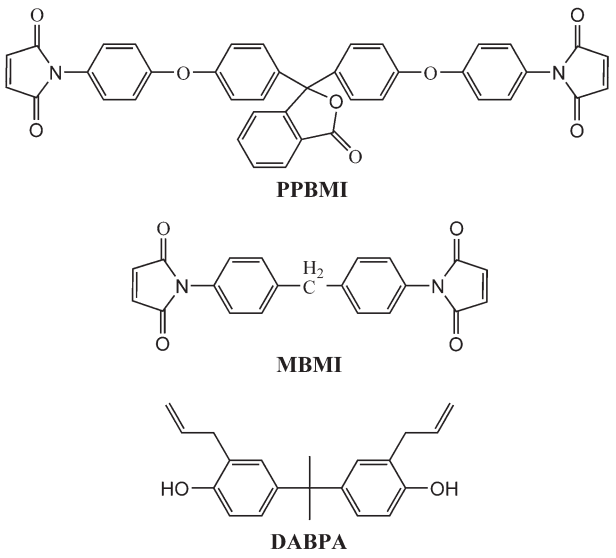

Figure 1. Chemical structure of PPBMI, MBMI, and DABPA.

rigorous application. Therefore, it is necessary to develop the novel resins based on a two-component MBMI/DABPA system.

In the previous research, we synthesized a chain-extended BMI monomer containing phthalide cardo structure (PPBMI).[27] Compared with other chain-extend BMI monomers,[14–17] PPBMI shows an advantageous combination of properties, such as good solubility, lower melting point and favorable cost, and thus it has a great future. Nevertheless, its high melt viscosity and high cure temperature are unfavorable factors for manufacture. To overcome these limitations, DABPA was chosen as reactive diluent and accelerant to prepare modified resin and the cure mechanism and kinetics were also investigated by FTIR and nonisothermal DSC in our previous work.[28]

The objective of this article was to gain a novel copolymer resin by introducing PPBMI into MBMI/DABPA system. The length of linkage chain between two polymerizable maleimide groups of PPBMI is bigger than that of MBMI, and the substitution of PPBMI for MBMI can further reduce the crosslink density of the cured network and improve further the toughness accordingly. In addition, the higher aromaticity of PPBMI will compensate for the reducing of the heat-resistant properties caused by the decreasing crosslink density. The curing characteristic, thermo-mechanical behavior, thermal stability, mechanical properties and moisture absorption behavior of the PPBMI/MBMI/DABPA blends were also investigated.

EXPERIMENTAL

Materials

Commercially available 2, 2'-diallyl bisphenol A (DABPA) and 4, 4'-dimaleimido diphenylmethane (MBMI) were provided by Jiangyou Electrical Material Company (Sichuan, China) and Fengguang Chemical Company (Hubei, China), respectively. 3,3-bis[4-(4-maleimido-phenoxy)phenyl]phthalide (PPBMI) was synthesized in our laboratory according to the reported method.[27] The structures of PPBMI, MBMI, and DABPA are shown in Figure 1.

Preparation of PPBMI/MBMI/DABPA Blends

The PPBMI/MBMI/DABPA prepolymers were prepared as follow: a crushed mixture of PPBMI and MBMI in controlled stoichiometry was dissolved in DABPA at 150°C under vigorous stirring with maleimide to allylphenol stoichiometry of 1:0.87, and then a homogeneous, visually transparent mixture was obtained. The mixture was degassed at 150°C under vacuum to remove trapped air and then poured directly into preheated (150°C) Teflon moulds and thermally cured in an air convection oven at 180°C for 1 h, 200°C for 2 h plus a post-cure period at 250°C for 6 h. Finally, the casting was removed from the mould and characterized.

PPBMI/MBMI/DABPA blends with PPBMI/MBMI molar ratios of 0:1, 1:9, 3:7, 5:5, 7:3, and 1:0 were designated as PM01, PM19, PM37, PM55, PM73, and PM10, respectively.

Characterization

Differential scanning calorimetry (DSC) measurements were conducted with an NETZSCH DSC 204 instrument. About 7–9 mg samples were used at a heating rate of 10°C/min under a flow of nitrogen (20 mL/min).

Dynamic mechanical analysis (DMA) was done on a TA Instruments Q800 DMA with an amplitude of 20 μm, driving frequency of 1.0 Hz, and a temperature ramp rate of 5°C/min in nitrogen atmosphere. The specimen was cut to dimensions of 40 mm × 6 mm × 2.5 mm for the single cantilever mode.

Thermogravimetric analysis (TGA) was performed on a Perkin-Elmer TGA-7 thermal analyzer and the sample (around 5 mg) was heated from 25 to 600°C at a heating rate of 20°C/min, under the purified nitrogen flow rate of 60 mL/min.

The fracture toughness of the cured epoxy resins was evaluated from the impact strength according to the GB/T 1843–1996. The tests were performed on the Izod impact testing machines (XJ-40A).

The fracture surfaces of impact specimens were analyzed by SEM (QUANTA200, FEI). The specimens were adhered to a SEM mount with conductive adhesive. The microscope was operated under 60Pa with accelerating voltage of 25 kV.

The water absorption rates were measured as follows: the sample, in the form of disk (20 mm in diameter and 2.5 mm in thickness), was dried in vacuo at 130°C until constant weight. Then the dried sample was immersed in a jar full of deionized water at desired temperature and periodically removed from the water, wiped down, and quickly weighed to an accuracy of 0.1 mg. The percentage of water absorbed by the specimens is calculated using the equation given below:

$$\%\ \text{Increase in weight} = (W_t - W_0)\,/\,W_0 \times 100 \qquad (1)$$

where W_0 is the weight of the dry specimen and W_t is the weight of the wet specimen at time t.

RESULTS AND DISCUSSION

Cure Behavior Studied by DSC

DSC is an effective thermal analysis technique, which can provide many useful thermal characteristics of a resin, such as

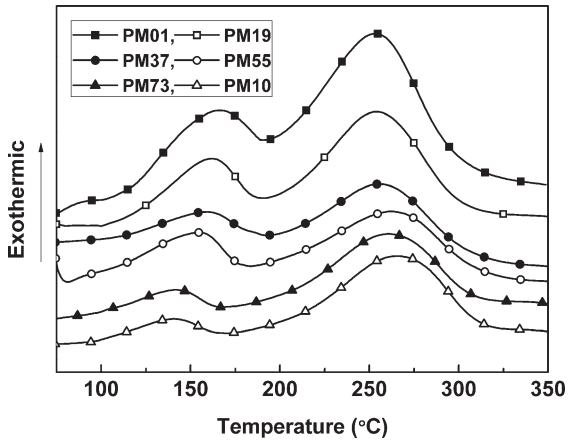

Figure 2. DSC curves of PPBMI/MBMI/DABPA systems.

melting point, cure temperature, enthalpy of the cure reaction, glass transition temperature (T_g), temperature of thermal decomposition. Herein, the reactivity of the PPBMI/MBMI/DABPA prepolymers was characterized by DSC at a heating rate of 10 K min^{-1} under a nitrogen atmosphere. The dynamic DSC thermograms are shown in Figure 2 and the analytical results are listed in Table I. All DSC curves show one main exothermic peak and a shoulder peak at a lower temperature, indicating different cure regimes. The exothermic peaks at 150°C is associated with the "ene" reaction between ally group and maleimide group and the exothermic peak located at 260°C is mainly ascribed to the Diels-Alder reaction, thermal rearrangement, thermal crosslinking as well as dehydration of the hydroxyl groups.[24,25] It is observed from the figure that the exothermic peaks at the lower temperature shift progressively to lower temperatures and become smaller with the PPBMI content. This may be ascribed to the increasing viscosity of the systems. The viscosity of the systems with higher PPBMI concentration is higher and increases more quickly as reaction progresses, in return, the higher viscosity traps reactive groups and makes "ene" reaction stop earlier. In fact, when the viscosity of the blend system is increased enough, through prolonging the time of prepolymerization at lower temperature, these exothermic peaks even can disappear. On the other hand, the exothermic peak at higher temperature shifts toward higher temperature and become broader as the PPBMI content increases. It may be attributed to the steric hindrance of bulky phthalide cardo structure in PPBMI, which reduces the mobility of the reactive site. During the thermal polymerization, the lower diffusion rate resulted in slower polymerization.

Table I. Characteristics Data of PPBMI/MBMI/DABPA Systems Evaluated from DSC Curves

Sample	PM01	PM19	PM37	PM55	PM73	PM10
T_i[a](°C)	115.7	113.2	111.9	114.3	114.2	113.5
T_{p1} [b](°C)	166.2	161.4	159	154.7	144.2	140.9
T_{p2} [c](°C)	252.1	254.1	256.3	262.2	262.7	265.4
T_f[d](°C)	302.5	302.9	304.5	305.7	306.3	310.2

[a] The initial curing temperature.
[b] The first exothermic transition temperature.
[c] The second exothermic transition temperature.
[d] The finial curing temperature.

Thermal Mechanical Properties Studied by DMA

The thermal mechanical behavior of cured PPBMI/MBMI/DABPA systems was investigated by dynamic mechanical analysis (DMA). Figures 3(a) and 4 show the temperature dependence of storage modulus (E') and loss tangent (tan δ) of the polymer and the characteristic data were listed in Table II. From Table II, it is obvious that the E's in the glassy region for all samples are around 3 GPa and unchanged with PPBMI content, whereas E's in the rubbery region decrease as PPBMI content is increased. According to the theory of rubber elastic, the

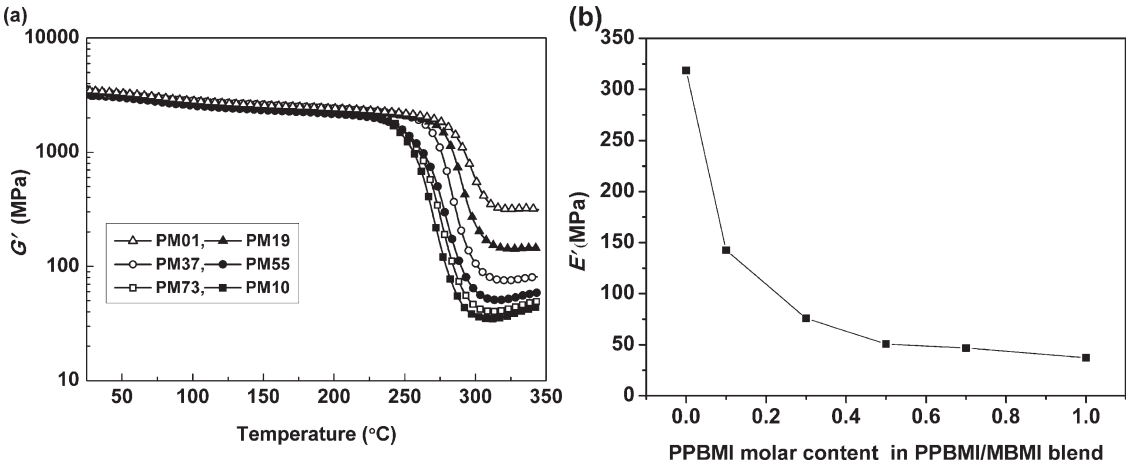

Figure 3. (a) storage modulus (E') of cured PPBMI/MBMI/DABPA systems; (b) E' in the rubbery plateau region versus PPBMI molar content in PPBMI/MBMI blend.

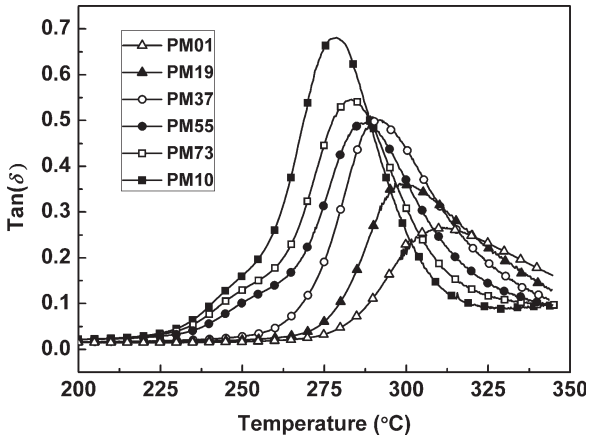

Figure 4. Damping factor (tan δ) of cured PPBMI/MBMI/DABPA systems.

crosslink density of a cured network can be approximated by the following derivative formula:[29]

$$M_c \cong \frac{3\rho RT}{E'} \quad (2)$$

where E' is the storage modulus in the rubbery region, R is the universal gas constant, ρ is the density, M_c is the average molecular weight of the chain segments between crosslink points, and T is the absolute temperature. By assuming that ρ is constant for all samples, the E' will be inversely proportional to M_c. Thus, the lower value of storage modulus in the rubbery plateau region is an indication of the enhanced length of the molecular chain segments between crosslink points. That is, the crosslink density of the cured resins reduced with PPBMI content. Figure 3(b) shows E's in the rubbery region firstly decreases drastically and then slowly as the PPBMI/MBMI molar ratio rises. The trend indicates addition of a small quantity of PPBMI can result in outstanding decrease of the crosslink density.

Table II. Characteristic Data of the DMA Thermograms for the Cured PPBMI/MBMI/DABPA Systems

	Storage modulus (MPa)		tan δ	
Sample	Glassy (50°C)	Rubbery (325°C)	T_g[a] (°C)	Peak height
PM01	3194	318.6	311	0.29
PM19	3167	142.6	299	0.36
PM37	3154	75.7	292	0.50
PM55	2995	50.8	286	0.50
PM73	3181	46.7	283	0.55
PM10	3109	37.3	277	0.68

[a] The temperature corresponding to the maximum of the tan δ peak

From tan δ-T curve in Figure 4, only one sharp and symmetrical tan δ peak for all cured resins is observed, indicating the formation of a homogeneous network structure of PPBMI/MBMI/DABPA. Additionally, as PPBMI content increases, tan δ peak shifts toward to lower temperature, peak value and temperature region (tan $\delta > 0.3$), which usually are used to characterize damping property, become bigger. Providing the temperature at the maximum of tan δ peak is identified as the glass transition temperature (T_g), T_g decreases with an increase in the concentration of PPBMI. This is due to the decreased crosslink density. Although the increased aromaticity of network favors the T_g, obviously the decrease of the crosslink density plays a dominant role. In the other hand, the present of bulky phthalide cardo increases the friction of molecular chain during network relaxation, which results in an increase of tan δ peak value.

Thermal Stability Studied by TGA

The thermal stability of the cocured systems was assessed by TGA, carried out in nitrogen atmosphere (see Figure 5). The degradation behavior was characterized in term of the initial decomposition temperature (T_i), temperature of 50% weight loss ($T_{50\%}$), temperature of maximum rate of decomposition (T_{max}) and char yield at 600°C, and the corresponding data are compiled in Table III. From an inspection of the TGA thermograms in Figure 7, all the formulations exhibited similar pattern of decomposition, but the rate of decomposition were highly dependent on the composition. The TGA data (Table III)

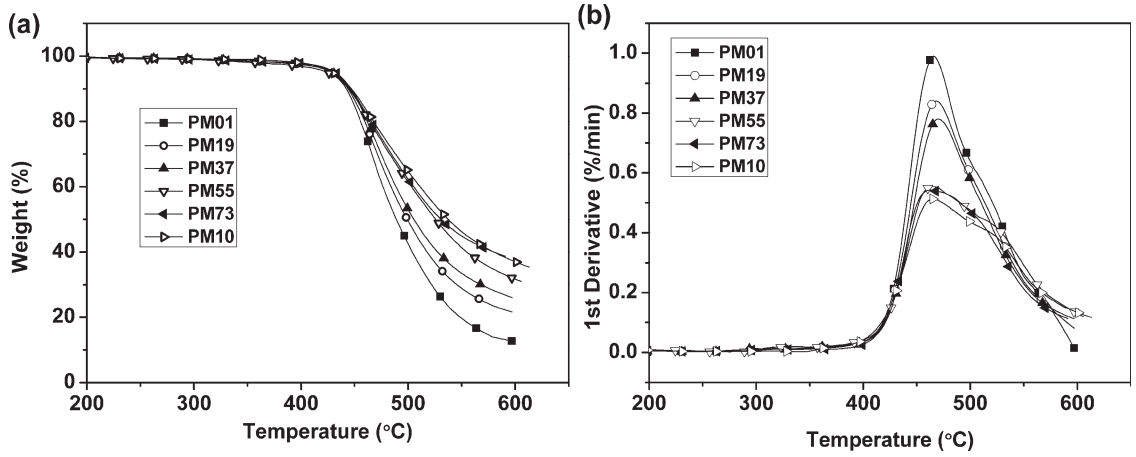

Figure 5. (a) TG and (b) DTG curves of cured PPBMI/MBMI/DABPA resins.

Table III. Thermal Decomposition Characteristics of the Cured PPBMI/MBMI/DABPA Systems

Sample	T_i[a] (°C)	$T_{50\%}$[b] (°C)	T_{mx}[c] (°C)	RW[d] (%)	E_{a1}[e] (kJ/mol)	$R_1{}^{2}$[f]	E_{a2}[g] (kJ/mol)	$R_2{}^{2}$[f]
PM01	426	488	466	12.7	281.3	0.987	83.9	0.997
PM19	427	498	467	21.6	271	0.991	82.9	0.993
PM37	429	505	470	26.1	265.1	0.993	82.9	0.99
PM55	424	525	463	30.9	252.3	0.99	87.6	0.998
PM73	431	532	459	37.3	262.7	0.984	85.2	0.995
PM10	431	546	464	36.9	244.9	0.985	83.5	0.998

[a] The initial decomposition temperature.

[b] Temperature at 50% weight loss.

[c] Temperature corresponding to the maximum rate of weight loss.

[d] Residual weight percentage at 600°C.

[e] The activation energy for the degradation in the temperature range 415–465°C.

[f] R^2, linear fit regression coefficient.

[g] The activation energy for the degradation in the temperature range 465–600°C.

indicated that the thermal stability was improved with enhanced concentration of PPBMI. Generally, higher crosslinked network is expected to possess relatively good thermal stability. However, the systems with higher PPBMI content result in reduced crosslink density according to above investigation. The possible explanation is that the increasing PPBMI content could reduce the relative concentration of the aliphatic chain in the network, which derived from the methylene, isopropyl, allyl groups. In other words, it is the reduced amount of weak heat-resistant network that is responsible for the increased thermal degradation temperature.

To evaluate the effect of composition on the thermal stability more detailed, the kinetic analysis of the thermal degradation process for all systems was performed following the rate expression for a nonisothermal reaction given as:

$$\frac{d\alpha}{dt} = k(1-\alpha)^n \tag{3}$$

where α, k, and n are the apparent conversion, the rate constant and the overall reaction order, respectively. The temperature dependence of the rate constant k may be described by the Arrhenius expression as follows:

$$k = A\exp\left(-\frac{E_a}{RT}\right) \tag{4}$$

Combining eqs. (3) and (4), and a heating rate $\beta = dT/dt$, the overall decomposition rate of polymer is given by:

$$\frac{d\alpha}{dT} = \frac{A}{\beta}\exp\left(-\frac{E_a}{RT}\right)(1-\alpha)^n \tag{5}$$

where α is the conversion at temperature T, dependent on the heating rate β, E_a is the apparent activation energy, A is the Arrhenius pre-exponential factor, and R is the universal gas constant.

Different kinetics expressions could be obtained by integrating eq. (5). Among them, a noted model is the Coats–Redfern (C–R) equation, expressed as

$$\ln\left[\frac{g(\alpha)}{T^2}\right] = \ln\left[\left(\frac{AR}{\beta E_a}\right)\left(1-\frac{2RT}{E_a}\right)\right] - \frac{E_a}{RT} \tag{6}$$

where $g(\alpha) = -\ln(1-\alpha)$ for $n = 1$ and when $n \neq 1$, $g(\alpha) = \left[1-(1-\alpha)^{1-n}\right]/(1-n)$.

For the degradation of crosslinked polymers, the mechanism of random scission of molecules dominates usually. Hence, a first order kinetics was assigned for the blending systems under investigation without serious error. Correspondingly, eq. (6) is expressed as:

$$\ln\left[\frac{-\ln(1-\alpha)}{T^2}\right] = \ln\left[\left(\frac{AR}{\beta E_a}\right)\left(1-\frac{2RT}{E_a}\right)\right] - \frac{E_a}{RT} \tag{7}$$

Based on eq. (7), the curves of $-\ln(1-\alpha)/T^2$ versus $1000/T$ were computed with conversion and shown in Figure 6. As a rule, they should present straight lines and the activation energy

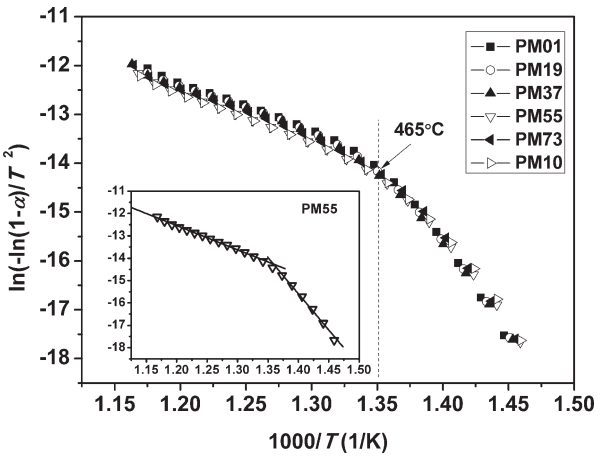

Figure 6. Kinetic plots of thermal decomposition of cured PPBMI/MBMI/DABPA resins by using Coats–Redfern equation.

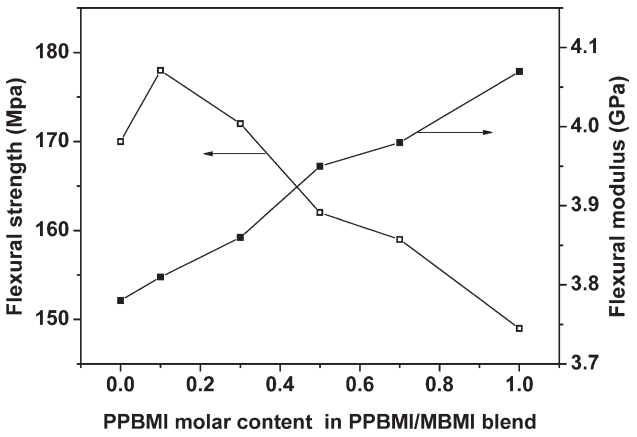

Figure 7. Flexural strength and flexural modulus of cured PPBMI/MBMI/DABPA resins versus PPBMI molar content in PPBMI/MBMI blend.

could be calculated from the slopes of fitting line and a good correlation coefficient confirms the validity of the assumed reaction order. However, differing from the patterns of the other thermosets, such as cured epoxy network[30] and polycyanurate,[31] the Coats–Redfern kinetic plots of the systems under study exhibits two regions of different slopes. Gouri et al.[12] observed the same phenomena when they carried out the kinetic analysis of the thermal degradation process of the BMI resins and the blend resins derived from thereof. They believed that the significant change in slops denoted two-step kinetics for the degradation and the kinetic parameters for the two steps could be independently calculated. In fact, a shoulder at the higher temperature side of the main peak appears in DTG curve and becomes bigger with the PPBMI content. Additionally, the temperature region corresponding to the change of slop was found to be close to the temperature of maximum rate of decomposition. These confirm the decomposition may occur through the two-step mechanism. The first step in the temperature range 415–465°C can be attributed to the degradation of the methylene and allyl group derived structures present in the network. The second step occurring in the 465–600°C range is most likely due to the degradation of the heterocyclic and aromatic structure and volatilization of the degraded products of the first step.

From the slope of the plots, activation energy was calculated and the results are compiled in Table III. It is observed that the activation energy for the first step of degradation gets reduced slightly with higher PPBMI content. This may result from the decrease of the crosslink points present in systems. The activation energy for the second step of degradation, independently of the composition, is only around 30–35% of that for the first step .These indicate the mass loss of the second step is mainly attributed to the volatilization of the degraded products of the first step.

Mechanical Properties and Morphology of Fracture Surface

Figure 7 shows the flexural strength and flexural modulus as a function of PPBMI/MBMI molar ratio. The flexural strength firstly increases and then decreases with PPBMI content, but the flexural modulus always increases. The increased rigidity contributed by PPBMI is responsible for the enhanced modulus. In addition, when the PPBMI/MBMI molar ratio is above 3:7, the viscosity of the modified resin outstandingly increases. Consequently, the defects, such as holes or air bubbles, are easy to form in the manufacture process. The present of the defects may be the main reason for the reduced flexural strength.

From Figure 8, it is observed that the impact strength tends to increase in the beginning and subsequently decreases on enhancing the PPBMI content. The phenomena may be explained in term of the crosslink density and the defect in the network. Generally, the crosslink density has a great influence on the toughening, and the toughness shows a maximum for intermediate crosslink density.[32] On the other hand, fracture initiation in glassy networks is in some way connected with the concentration of defects, which are likely to take part in embrittlement of the glassy polymers. The decrease of the flexural strength has indicated the enhanced defects in the system with higher PPBMI content.

Figure 9 exhibits the SEM image of the fracture surface of some samples. It can be seen that PM01 and PM37 systems show similar fracture surface, but rougher fracture surface with increasing PPBMI content. Compared with PM01 and PM37 systems, the fracture surface of PM10 system is smoother. In Figure 9(d), some light spots presented on the fracture surface of PM10 system are observed. This may be another evidence for the presence of the defect.

Moisture Absorption Behavior

The absorption and diffusion of moisture in BMI resin has been the focus of interest, because the absorbed moisture has many detrimental effects on the properties of cured products.[33,34] It was reported that the absorbed moisture, acting as a very effective plasticizer, decreased the strength and elastic modulus, substantially lowered the glass transition point and strongly deteriorated the dielectric properties. Therefore, it is important to probe the approach to reduce moisture uptake.

Figure 10 presents the water absorption curves of the cocured resins in boiling water as a function of immersion time. It is apparent that all cured resins have similar diffusion behavior, with water uptake initially increasing fast and eventually

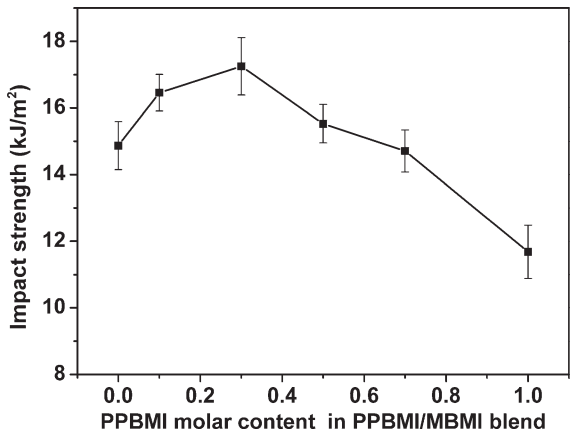

Figure 8. Impact strength of cured PPBMI/MBMI/DABPA resins versus PPBMI molar content in PPBMI/MBMI blend.

Applied Polymer SCIENCE

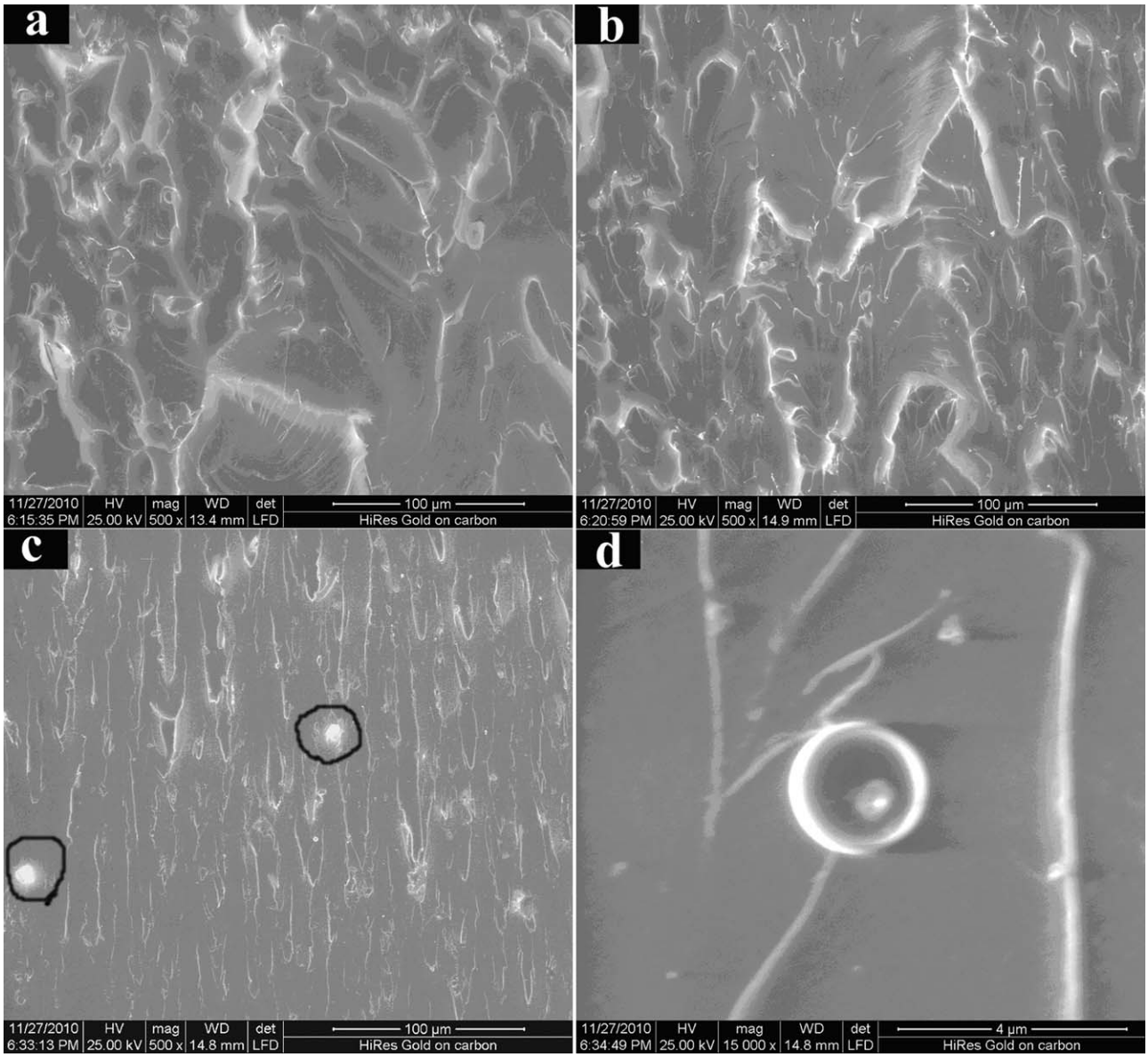

Figure 9. SEM images of failed surfaces of cured PPBMI/MBMI/DABPA systems (a)PM01 system; (b)PM37 system; (c)PM10 system; (d) PM10 system.

reaching a plateau with the immersion time. From the trend of the data, there appears to be a strong link between the PPBMI content of the blend and the moisture absorption. Those blends containing large quantities of PPBMI display markedly lower equilibrium water content and initial rate of water absorption. This may be ascribed to the decrease of the relative amount of hydrophilic groups (such as hydroxyl group, carbonyl group) per volume unit in the network with increasing PPBMI content.

CONCLUSIONS

PPBMI/MBMI/DABPA resins with varying PPBMI to MBMI molar ratio were developed. The cure behavior monitored using DSC showed that the main exothermic peaks shift progressively toward higher temperatures with the PPBMI content. The DMA

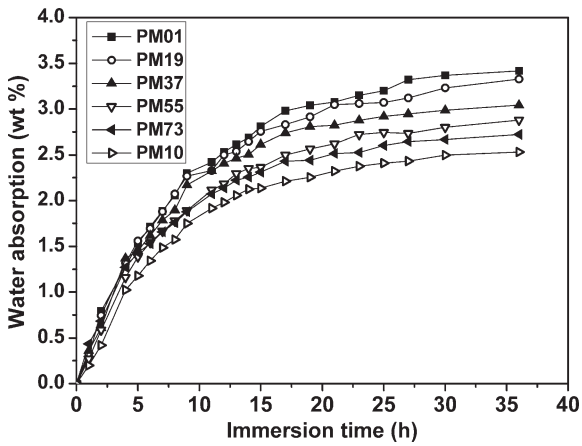

Figure 10. Water absorption curves of cured PPBMI/MBMI/DABPA systems in boiling water.

results showed that the storage modulus (E') in the glassy region is in independent of the blend composition but E' in the rubbery plateau and glass transition temperature (T_g) both decreased as the PPBMI content was enhanced. The TGA showed similar pattern of single stage decomposition. The systems with higher PPBMI content exhibited a marginal improvement in thermal stability. Contrary to the apparent single step degradation manifested in TGA, the non-isothermal kinetic plots showed two major sectors for all the systems. The activation energy (E_a) for the first step of degradation in the temperature range 415–465°C reduced slightly with PPBMI content and E_a for the second step of degradation in the temperature range 465–600°C is only around 30–35% of that for the first step. Mechanical properties of the blend systems varied with the composition and the system with PPBMI/MBMI molar ratio equal to 3:7 possessed the maximum impact strength. The equilibrium water content and the initial rate of water absorption decreased as PPBMI content was increased.

ACKNOWLEDGMENT

The financial support from the National Defense 12-th 5-year Fundamental Research Program (No.A3520110001), Scientific Research Foundation for Young Teachers of Shenyang Aerospace University (nos. 12YB23, 201211Y), Liaoning Provincial Science and Technology Plan Project (no. 2007403009) and Innovative Research Team Program in University of Liaoning Education Department (no. LT2010083) is gratefully acknowledged.

REFERENCES

1. Stenzenberger, H. D. *Adv. Polym. Sci.* **1994**, *117*, 165.
2. Mison, P.; Sillion, B. *Adv. Polym. Sci.* **1999**, *140*, 137.
3. Swan, M.; Pritchard, G. *J. Mater. Sci. Lett.* **1992**, *11*, 1443.
4. Abbate, M.; Martuscelli, E.; Musto, P.; Ragosta, G. *J. Appl. Polym. Sci.* **1997**, *65*, 979.
5. Gopala, A.; Wu, H.; Harris, F.; Heiden, P. *J. Appl. Polym. Sci.* **1998**, *69*, 469.
6. Hamerton, I.; Klewpatinond, P. *Polym. Int.* **2001**, *50*, 1309.
7. Satheesh, C. M.; Krishna, M.; Salini, K.; Rai, K. S. *Int. J. Polym. Sci.* **2010**, 1.
8. Hopewell, J. L.; Georgeb, G. A.; Hill, D. J. T. *Polymer* **2000**, *41*, 8221.
9. Donnellan, T. M.; Roylance, D. *Polym. Eng. Sci.* **1992**, *32*, 409.
10. Yen, H. J.; Liou G. S. *J. Mater. Chem.* **2010**, *20*, 4080.
11. Fang, Q.; Ding, X. M.; Wu, X. Y.; Jiang, L. X. *Polymer* **2001**, *42*, 7595.
12. Gouri, C.; Nair, C. P. R.; Ramaswamy, R.; Ninan, K. N. *Eur. Polym. J.* **2002**, *38*, 503.
13. Rozenberg, B. A.; Dzhavadyan, E. A.; Morgan, R.; Shin E. *Polym. Adv. Technol.* **2002**, *13*, 837.
14. Wang, C. S.; Leu, T. S. *J. Appl. Polym. Sci.* **1999**, *73*, 833.
15. Hu, Z.; Li, S.; Zhang, C. *J. Appl. Polym. Sci.* **2008**, *107*, 1288.
16. Hwang, H. J.; Li, C. H.; Wang C. S. *Polym. Int.* **2006**, *55*, 1341.
17. Tang, H. Y.; Song, N. H.; Gao, Z. H.; Zhou, Q. F. *Polymer* **2007**, *48*, 129.
18. Musto, P.; Martuscelli, E.; Ragosta, G.; Russo, P.; Scarinzi, G.; Villano, P. *J. Mater. Sci.* **1998**, *33*, 4595.
19. Kumar, A. A.; Alagar, M.; Rao, R. M. V. G. K. *Polymer* **2002**, *43*, 693.
20. Zhou, B. X.; Huang, Y. J.; Zhang, X. H.; Fu, Z. S.; Qi, G. R. *Polym. Eng. Sci.* **2009**, *49*, 1525.
21. Hwang, H. J.; Li, C. H.; Wang, C. S. *Polymer* **2006**, *47*, 1291.
22. Lin, R. H.; Lu, W. H.; Lin, C. W. *Polymer* **2004**, *45*, 4423.
23. Takeichi, T.; Saito, Y.; Agag, T.; Muto, H.; Kawauchi, T. *Polymer* **2008**, *49*, 1173.
24. Morgan, R. J.; Shin, E. E.; Rosenberg, B.; Jurek, A. *Polymer* **1997**, *38*, 639.
25. Mijovic, J.; Andjelic, S. *Macromolecules* **1996**, *29*, 239.
26. Phelan, J. C.; Sung, C. S. P. *Macromolecules* **1997**, *30*, 6845.
27. Xiong, X. H.; Chen, P.; Yu, Q.; Zhu, N. B.; Wang, B. C. *Polym. Int.* **2010**, *59*, 1665.
28. Xiong, X. H.; Chen, P.; Zhang, J. X.; Yu, Q.; Wang, B. C. *Thermochimica Acta* **2011**, *514*, 44.
29. Li, J. Y.; Chen, P.; Ma, Z. M.; Ma, K. M.; Wang, B C. *J. Appl. Polym. Sci.* **2009**, *111*, 2590.
30. Guo, B. C.; Jia, D. M.; Cai, C. G. *Eur. Polym. J.* **2004**, *40*, 1743.
31. Nair, C.P. R.; Mathew, D.; Ninan, K. N. *Adv. Polym. Sci.* **2001**, *155*, 1.
32. He, S. J.; Shi, K. Y.; Bai, J.; Zhang, Z. K., *Polymer* **2001**, *42*, 9641.
33. Bao, L. R.; Yee, A. F.; Lee, C. Y. C. *Polymer* **2001**, *42*, 7327.
34. Chaplina, A.; Hamertonb, I.; Hermanb, H.; Mudhar, A. K.; Shawa, S. J. *Polymer* **2000**, *41*, 3945.